Title

Pathology of high current density stimulation in the retina

Permalink

https://escholarship.org/uc/item/06v6051p

Authors

Colodetti, L
Weiland, JD
Colodetti, S
et al.

Publication Date

2023-12-10

Peer reviewed

Pathology of damaging electrical stimulation in the retina

L. Colodetti, J.D. Weiland*, S. Colodetti, A. Ray, M.J. Seiler, D.R. Hinton, M.S. Humayun

Department of Ophthalmology, University of Southern California, 1355 San Pablo Street, Room 160, Los Angeles, CA 90033, USA

Abstract

The goal of this study was to examine the characteristics of electrically induced retinal damage. A retinal prosthesis must be both effective and safe, but most research related to electrical stimulation of the retina has involved measures of efficacy (for example, stimulus threshold), while relatively little research has investigated the safety of electrical stimulation. In this study, a single platinum microelectrode was inserted into the vitreous cavity of normally-sighted adult Long Evans pigmented rats. In one group of animals, no contact was made between the electrode and the retina and current pulses of 0.05 ($n = 3$) and 0.2 ($n = 6$) μC/phase were applied. In a second group, visible contact (slight dimpling of the retina) was made between the electrode and the retina and current pulses of 0.09 ($n = 4$) μC/phase were applied. In both cases, stimulus pulses (biphasic, cathodic first, 1 ms/phase) were applied for 1 h at 100 Hz. Also, control experiments were run with no electrical stimulation with retina contact ($n = 4$) and with no retinal contact ($n = 3$). After stimulation, the animal was survived for 2 weeks with ocular photography and electroretinography (ERG) to document changes. During the follow-up period, retinal changes were observed only when the electrode contacted the retina, with or without electrical stimulation. No difference was noted in ERG amplitude or latency comparing the test eye to the stimulated eye. Histological analysis was performed after sacrifice at 2 weeks. A semi-quantitative method for grading 18 features of retina/RPE/choroidal appearance was established and integer grades applied to both test and control eyes. Using this method and comparing the most severely affected area (highest grade), significant differences ($p < 0.05$) were noted between experiments with retinal contact and without retinal contact in all features except inner nuclear layer thickness. No difference was noted within a group based on the intensity of electrical stimulus applied. The size of the affected area was significantly larger with both retinal contact and electrical stimulation compared to with retinal contact alone. We conclude that mechanical pressure alone and mechanical pressure with excessive electrical stimulation causes damage to the retina but that electrical stimulation coupled with mechanical pressure increases the area of the damage.
© 2007 Elsevier Ltd. All rights reserved.

Keywords: retinal prosthesis; electrical stimulation; retina; retinal degeneration

1. Introduction

An electronic retinal prosthesis has been proposed to restore vision in patients with blindness due to retinitis pigmentosa (RP) and age- related macular degeneration (Zrenner, 2002; Weiland et al., 2005). In both conditions, photoreceptor death ultimately leads to significant loss in visual acuity and in many cases blindness. Although the wiring of the retina is altered with progressive degeneration (Marc et al., 2003), inner retina neurons are still present (Stone et al., 1992; Santos et al., 1997; Humayun et al., 1999). Retinal prostheses are designed to create the sensation of vision by activating inner retina neurons with small pulses of electricity. This stimulation results in depolarization of the cells and the initiation of retinal ganglion cell action potentials, which the visual system perceives as a light stimulus at the retina. The principle of electrical activation of sensory systems is well established by years of experimentation and by the success of the cochlear implant. Clinical trials of prototype retinal prostheses have demonstrated that subjects see light in response to electrical stimulation and that simple visual tasks can be performed (Mahadevappa et al., 2005; Hornig et al., 2006; Zrenner et al., 2006). Despite the many technological obstacles to producing a device that

interfaces with the neural retina, potential advantages to this approach include the applicability to all forms of photoreceptor degeneration.

The purpose of this study was to investigate the pathology of retinal damage due to high charge density stimulation. The need for this investigation stems from the fact that a retinal prosthesis must be both effective and safe, but most of the biological research in retinal prostheses has focused on the issue of effectiveness, including electrophysiology in animal models and psychophysics in human test subjects (Rizzo et al., 2004; Mahadevappa et al., 2005; Sekirnjak et al., 2006). While a few studies have shown that low levels of stimulation are safe (Guven et al., 2005; Pardue et al., 2005), no study has investigated the pathology of damage created by electrical stimulation of the retina. It is important to study the effects of high charge density stimulation, since data from human clinical trials has not shown any decrease in threshold charge related to decreased electrode diameter (Guven et al., 2006). Increasing the resolution of a retinal prosthesis may require smaller electrodes that can be densely placed in contact in the central retina. If electrode sizes shrink, but stimulus charge stays constant, charge density will increase.

2. Materials and methods

2.1. Animals

All animal experiments adhered to Association for Research in Vision and Ophthalmology guidelines and were approved by the University of Southern California Institutional Animal Care and Use Committee. Twenty adult Long Evans pigmented rats were included in this study (age 3−7 months) with experiments performed on one eye in each animal.

2.2. Experimental groups

There were two experimental groups: Group 1 (stimulating electrode near, but not contacting the retina) and Group 2 (stimulating electrode contacting the retina). Group 1 was divided in sub-groups 1A (3 rats), 1B (3 rats), 1C (6 rats) using 0.00, 0.05 and 0.2 μC of charge per phase, respectively. Group 2 was divided in sub-groups 2A (4 rats) and 2B (4 rats) of 0.00 and 0.09 μC of charge/phase, respectively. These levels were chosen to be in the range of stimulus levels reported for human clinical trials (Mahadevappa et al., 2005). The timing of the pulse was the same for all experiments: 1 ms cathodic, 1 ms delay, 1 ms anodic, applied at 100 pulses/s. The corresponding charge density was estimated to be 0.05 μC = 0.55 mC/cm^2, 0.09 μC = 1 mC/cm^2, and 0.2 μC = 2.2 mC/cm^2, based on the geometry of the stimulating electrode (description of electrode is given below). Charge/phase (not charge density) is used to describe the stimulus in this paper, since the electrodes were hand-made and had some variability in surface area (±5%, based on estimates from manufacturer, see next paragraph). These charge densities were above the safe limit for chronic stimulation for platinum (Brummer et al., 1983), since

the intent of the study was to study effects of high charge density stimulation.

2.3. Electrical stimulation electrode and system

The stimulating electrode was the inner pole of a concentric bipolar Pt/Ir electrode (inner pole of diameter 75 μm, model CBDRG75, FHC Inc., Bouidain, ME, USA) (Fig. 1), similar to that used in other studies. (Rizzo et al., 2004; Shah et al., 2006) The inner pole had a rounded tip (roughly hemispherical) and an estimated surface area of 9.35×10^{-5} cm^2 (based on a hemispherical surface area of 8.9×10^{-5} cm^2 + 5% for error due to manufacturing). No assumptions were made about the oxidation state of the platinum surface. A biphasic voltage pulse was generated using a stimulus generator (STG 2008, Multichannel Systems, Reutlingen, Germany). The voltage pulse was fed to an analog voltage-to-current converter (Model 2200, A-M Systems, Carlsborg, WA, USA). The output of the converter was a charge-balanced current pulse which was delivered to the electrode. The direct current (DC) offset control of the stimulus isolator was manually adjusted to minimize DC and to ensure no gross changes in electrode voltage, indicative of charge accumulation due to DC offset. In earlier studies not reported here, where DC offset was not adjusted prior to testing, the voltage drop was wildly drifting and retina damage was widespread; results consistent with an imbalance in stimulus charge. Although the offset current was not measured directly, the leak current was estimated to be less than 5 nA. From voltage waveforms (see online supplement), the DC offset was less than 100 mV, as measured directly from the gradations on the oscilloscope. Assuming a low frequency impedance of at least 20 MΩ (Fig. 6), a 5 nA estimate follows from Ohm's law, $I = V/R$. The precision of the voltage measurement is limited by the input impedance of the oscilloscope. Stimulus was applied for 60 min. The voltage drop across the electrode was continuously monitored (TDS 1002 digital oscilloscope or TDS 5043B storage digital oscilloscope, Tektronix Inc., Beaverton, OR, USA) to ensure that the stimulus signal was being applied.

In addition to monitoring the electrode voltage as described above, in a subset of later experiments, a more extensive battery of electrochemical tests were done to assess more subtle electrode changes due to pulsing. This is important since large changes in the electrode properties would confound the results due to change in the experimental conditions. Tests including open-circuit potential, cyclic voltammetry and impedance spectroscopy were carried out on the electrode. The open-circuit potential and cyclic voltammogram data were used to determine whether or not an oxide layer had formed on the electrode surface. The impedance data were used to ensure the continuity of the electrode circuitry. All measurements were made in a three-cell configuration in 0.1 M phosphate-buffered saline with a silver/silver chloride reference electrode and a platinum counter electrode. A commercial potentiostat was used for these measurements (FAS1 potentiostat, framework version 4.30, Gamry Instruments Inc., Warminster, PA, USA). The electrode tip was cleaned with distilled water before conducting the tests.
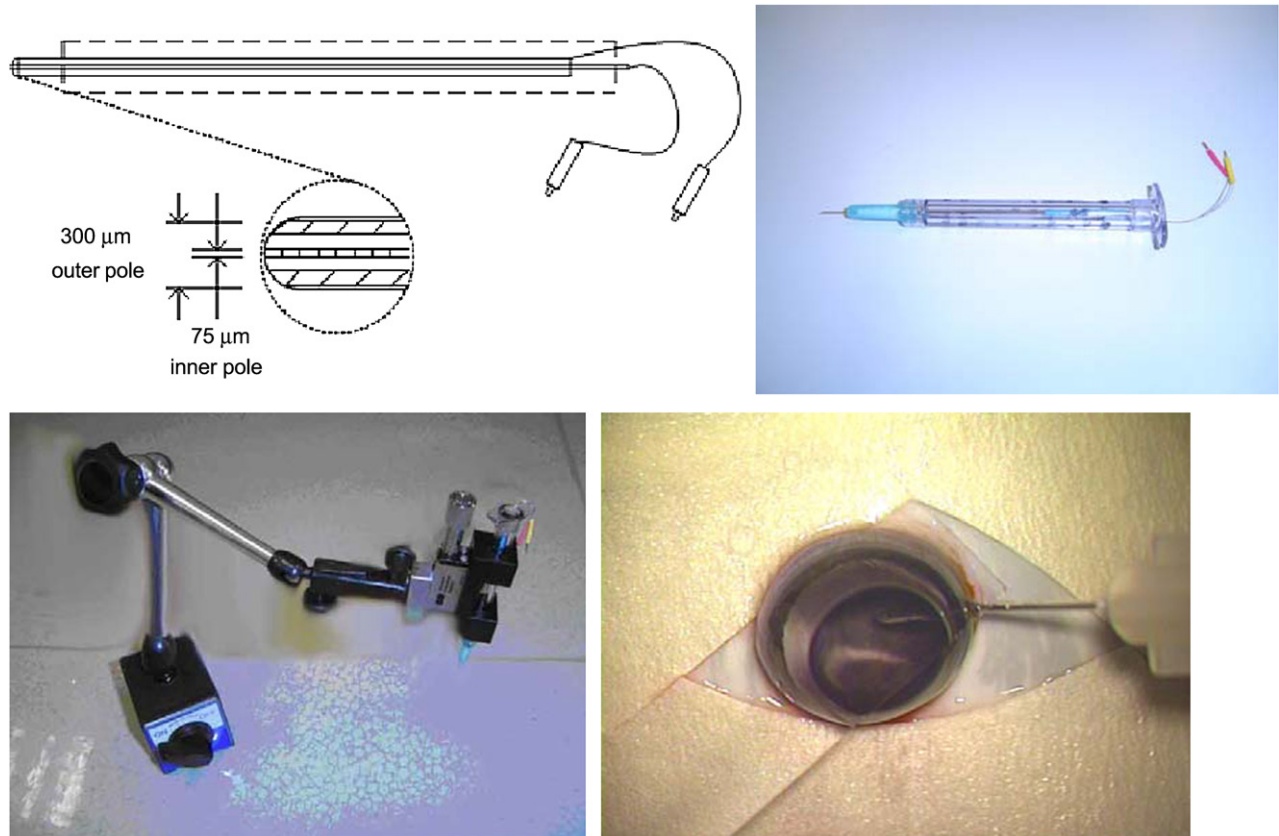
Fig. 1. Electrode and positioning. Upper left: Electrode diagram from FHC, Inc. showing detail of electrode tip. Upper right: The electrode was inserted in a syringe to facilitate handling. Lower left: The articulating arm holds the electrode in position after manual placement near the retina. The micromanipulator was used to advance the electrode near the retina or in contact with the retina. Lower right: A glass cover slip on the proptosed rat eye allows viewing of the electrode tip (view through a surgical microscope).

2.4. Anesthesia

Anesthesia was achieved by intramuscular injection of 4 parts ketamine hydrochloride 50–90 mg/kg 10% (Ketaset, Fort Dodge Animal Health, Fort Dodge, IA, USA) and 1 part xylazine 2% 5–10 mg/kg (X-ject E, Phoenix Scientific Inc., St. Joseph, MO, USA). One full dose was given initially and half doses every 30 min until the end of the procedure.

2.5. Surgical procedure

The eye was dilated with one drop each of 1% tropicamide (Tropicacyl, Akorn Inc., Buffalo Grove, IL, USA) and 2.5% phenylephrine (AK-Dilate, Akorn Inc.). The rat was anesthetized and positioned on a heater pad set to 37 °C to maintain body temperature. The eye was proptosed through a 4 × 4 mm hole of a 2 × 2 cm section of a sterile latex surgical glove to improve surgical exposure of the eye. A sterile drape was pulled tightly over the rat head and fixed to the table to minimize head and eye motion during the procedure. The fundus was viewed through an operating microscope. The retina could be viewed in focus by slightly flattening the cornea with an 18 × 18 mm glass coverslip (Fig. 1). A needle electrode (for stimulus current return) was inserted subcutaneously in the back of the rat.

A temporal sclerotomy was made (using a 27-gauge needle) approximately 0.5 mm from the limbus. The angle of the needle relative to the sclera was approximately 60° (relative to the anteroposterior axis of the eye) to avoid hitting the lens. The stimulating electrode (described above) was packaged in a 30-gauge cannula, mounted in a 1 cc syringe for handling (Fig. 1), and attached to a single-axis translational micropositioner stage on an articulating arm. The articulating arm was used for gross positioning of the electrode close to the retina. After manually positioning and fixing the articulating arm, the micropositioner was used to advance the electrode to its final position. It was clearly observable when the electrode contacted the retina since a slight dimpling of the retina could be seen. To position the electrode close to the retina without producing an observable dimpling, the shadow cast on the fundus by the microelectrode was used to estimate proximity. The electrode impedance was checked to verify the integrity of the connections. In test groups with electrical stimulation, current pulses were applied for 1 h. The microscope light was turned off unless needed to view the fundus. Every 15 min, the position of the electrode was checked by indirect ophthalmoscopy. A timer was used to track the accumulated stimulus time. After completion of the treatment, the electrode was removed. The small sclerotomy was self sealing. Topical antibiotic ointment was administered after procedure.

2.6. Diagnostic procedures

Diagnostic procedures were performed on the test and control eyes of all rats pre-operatively and 2 weeks post-operatively to assess the general health of the ocular structures. For all diagnostic procedures, the pupils were dilated and the animal anesthetized as described earlier.

2.6.1. Ocular photography

Color pictures and fluorescein angiograms (FA) were taken of the back of the eye using a handheld fundus camera (Model K9L29 Genesis, Kowa Co. Ltd., Tokyo, Japan). For fluorescein angiography (FA), 1–2 ml of fluorescein dye (AK-Fluor 10%, Akorn Inc.) was injected intravenously and photos were taken within 30 s of injecting the dye, at 1, 3 and 5 min.

2.6.2. Electroretinography

In a subset of experiments, full field flash electroretinography (ERG) was performed (Espion console D112, Espion Diagnostics LLC, Littleton, MA, USA). Rats were dark adapted for 30 min prior to testing.

2.6.3. Fundus examination

This examination was performed with the animal restrained or anesthetized. An indirect ophthalmoscope (XONIX Stereoscope, Xonix Inc., MA, USA) with a Volk 20D lens was used to view the retina at 1 and 2 weeks post-operatively.

2.7. Tissue processing

All eyes were fixed and processed with the same protocol. The animal was euthanized 2 weeks post-operatively and both eyes enucleated. The eyes were immersion-fixed in Bouin's fixative on a shaker for 2–5 h at room temperature (or overnight at 4 °C). Eyes were washed three times (at least 5 min each) with 80% ethanol and stored in 80% ethanol at 4 °C. Eye cups were dissected in 80% ethanol to obtain cross sections through the area of interest, and then embedded in paraffin, continuing from 80% ethanol. Microtome sections were cut from the embedded tissue in 5 μm steps, in serial order. About 100 slides were prepared in this fashion for each eye, with 3–6 sections on each slide. Every 5th slide was stained with hematoxylin/eosin. The unstained sections were stored at room temperature for later immunohistochemistry analysis (see below).

2.8. Immunohistochemistry

For identification of glial cells, a polyclonal rabbit anti-GFAP (Chemicon International Inc., Temecula, CA, USA) was used. Retinal sections from 1 normal and 10 treated eyes were deparaffinized, rehydrated and treated with 0.5% hydrogen peroxide to block any endogenous peroxidase activity. After washing, the sections were treated with 0.01 M citrate buffer (pH 6.0) for 20 min at 95–97 °C for antigen retrieval. The slides were left to cool down to room temperature, rinsed with phosphate-buffered saline (PBS), followed by blocking solution (20% goat serum in PBS, 1% BSA for 30 min at room temperature), and overnight incubation at 4 °C with the primary antibody (1:10,000). After several washes, slides were incubated with biotinylated secondary antibody (goat anti-mouse serum; 1:200; Vector Laboratories, Burlingame, CA, USA) and then with horseradish avidin–biotin complex (ABC solution; Vector Laboratories), each incubation step for 30 min at room temperature. The HRP–ABC complex was detected using a Vector DAB kit.

2.9. Histological evaluation

Slides of the test eyes were evaluated for structural changes using light microscopy by a masked examiner. Results were evaluated by pre-established evaluation categories and grading scales for each parameter. The characteristics evaluated in retinal tissue were: pigmentary changes, gliosis, outer nuclear layer thickness, inner nuclear layer thickness, ganglion cell morphology and number, outer plexiform layer (OPL) thickness, inner plexiform layer (IPL) thickness, photoreceptor inner segment morphology, photoreceptor outer segment morphology, and cellular infiltrates in subretinal space. The histological characteristics evaluated in the retinal pigment epithelium (RPE) layer were: proliferation, increase or decrease in pigmentation, RPE loss, RPE atrophy, and RPE hypertrophy. The characteristics evaluated in the choroids were: atrophy of choriocapillaris and choroidal larger vessels. Each of these parameters was graded semi-quantitatively as none/minor, minimal, mild, moderate, and severe changes. The most severely affected area of lesion for each case was selected and graded, using the pre-established criteria. An example of a graded slide is shown in Fig. 2. The size of the lesion in the stimulated and non-stimulated cases in Groups 2A and 2B was compared by measurements done in hematoxylin/eosin-stained slides. Lesion size was compared using a Student *t*-test. Histological
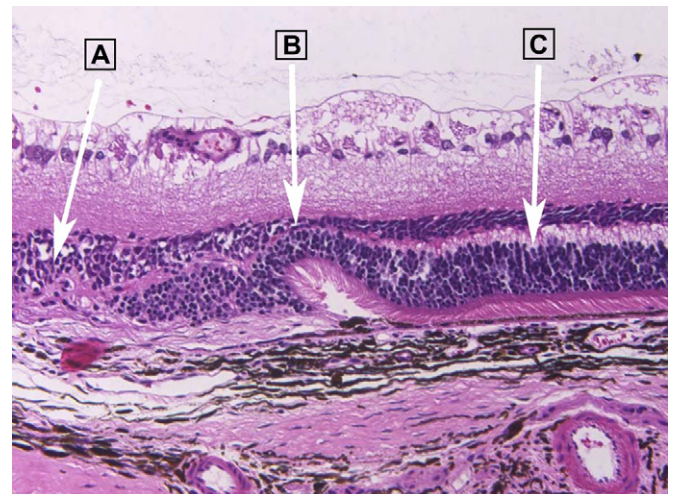

Fig. 2. Outer nuclear layer: example of the evaluation criteria. (A) Severe changes (score 4) thickness of outer nuclear layer < 4 cell layers. (B) Moderate changes (score 3) thickness of outer nuclear layer reduced to 4–5 cell layers. (C) None or minor changes (score 0) with no loss of photoreceptors cells. Results were evaluated by pre-established evaluation categories and grading scales for each parameter.

grading parameters were compared with a Wilcoxon rank sum. In both cases, a significance level of 0.05 was used.

3. Results

3.1. Operative and post-operative observations

The electrode could be positioned routinely without causing retinal detachment or intraocular bleeding. Small pre-retinal hemorrhage was noted in two rats at the end of the surgery but this was resolved after 2 weeks. Due to post-operative corneal haziness, ocular photography could only be obtained in a limited number of rats; however, indirect examinations were performed in all rats. The indirect exam observations were consistent within groups. All rats in Group 1 (no contact, 0, 0.05, and 0.2 µC stimulus) showed no differences between test and control eyes. A color photo of a Group 1 rat is shown in Fig. 3. Group 2A (retinal contact, no stimulation) showed a rounded hypopigmentation area surrounded by blood, in the area where the electrode contacted the retina (Fig. 3). In Group 2B (retinal contact and electrical stimulation) a large hypopigmentation area was observed where the retina was compressed and electrical stimulus was applied; in addition, small scattered hyperpigmentation areas were observed (Fig. 3).

Baseline FAs were normal in all rats. Post-operative FA could be obtained only in two rats from Group 2 and three rats in Group 1 (Fig. 4). In Group 2A, fluorescein angiography at 2 weeks post-operatively revealed hyperfluorescence surrounded by hypofluorescence in the area where the retina was contacted by electrode. In Group 2B, a large area of weak hyperfluorescence was surrounded by a smaller area of strong hyperfluorescence. This area of strong hyperfluorescence was in the same area where the electrode was contacting the retina. In Groups 1A, 1B and 1C, there were no indicators of choroidal
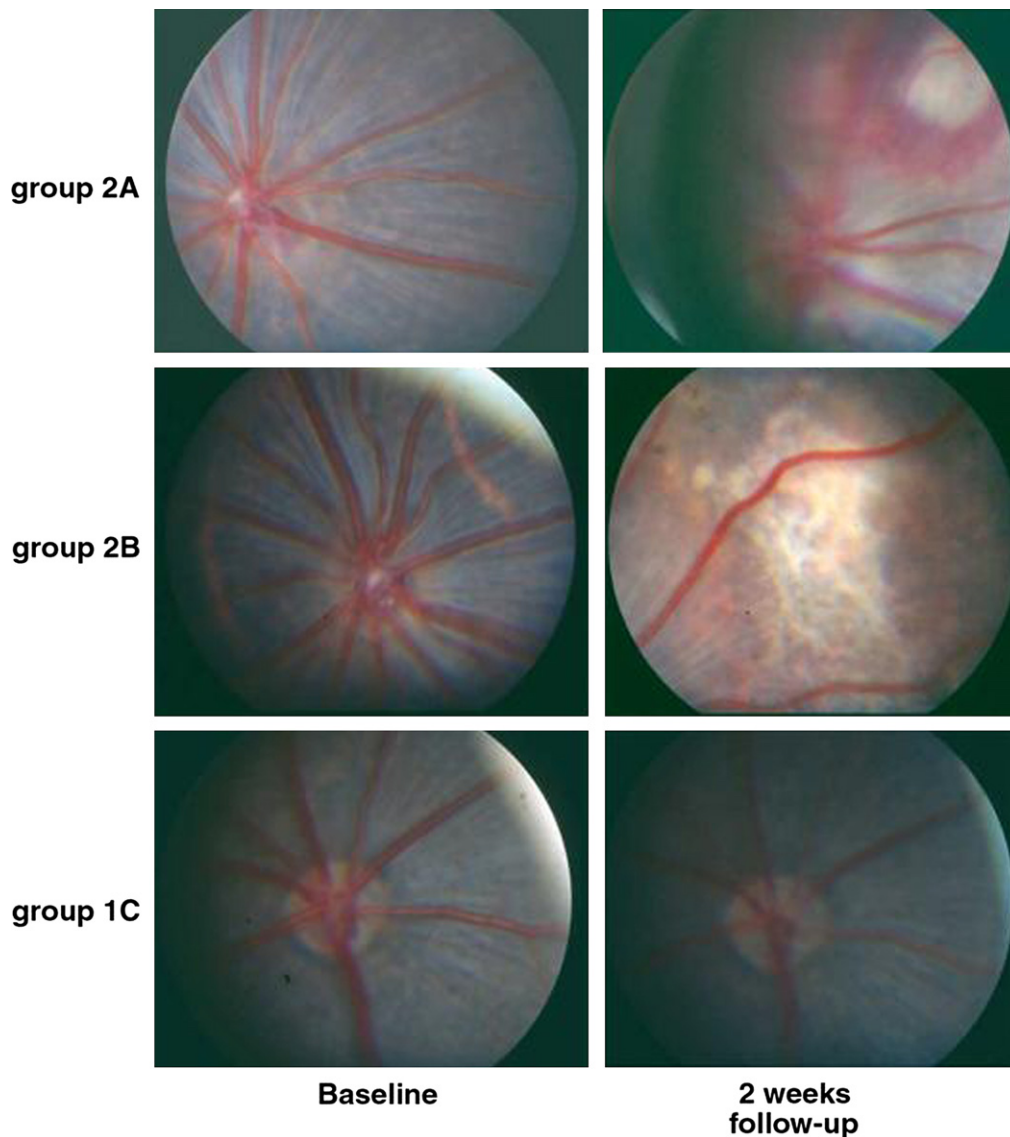

Fig. 3. Fundus photography results. Group 2A: Hypopigmentation area surrounded by hemorrhage. Group 2B: large Hypopigmentation area and hyperpigmentation area. Group 1C: Normal.
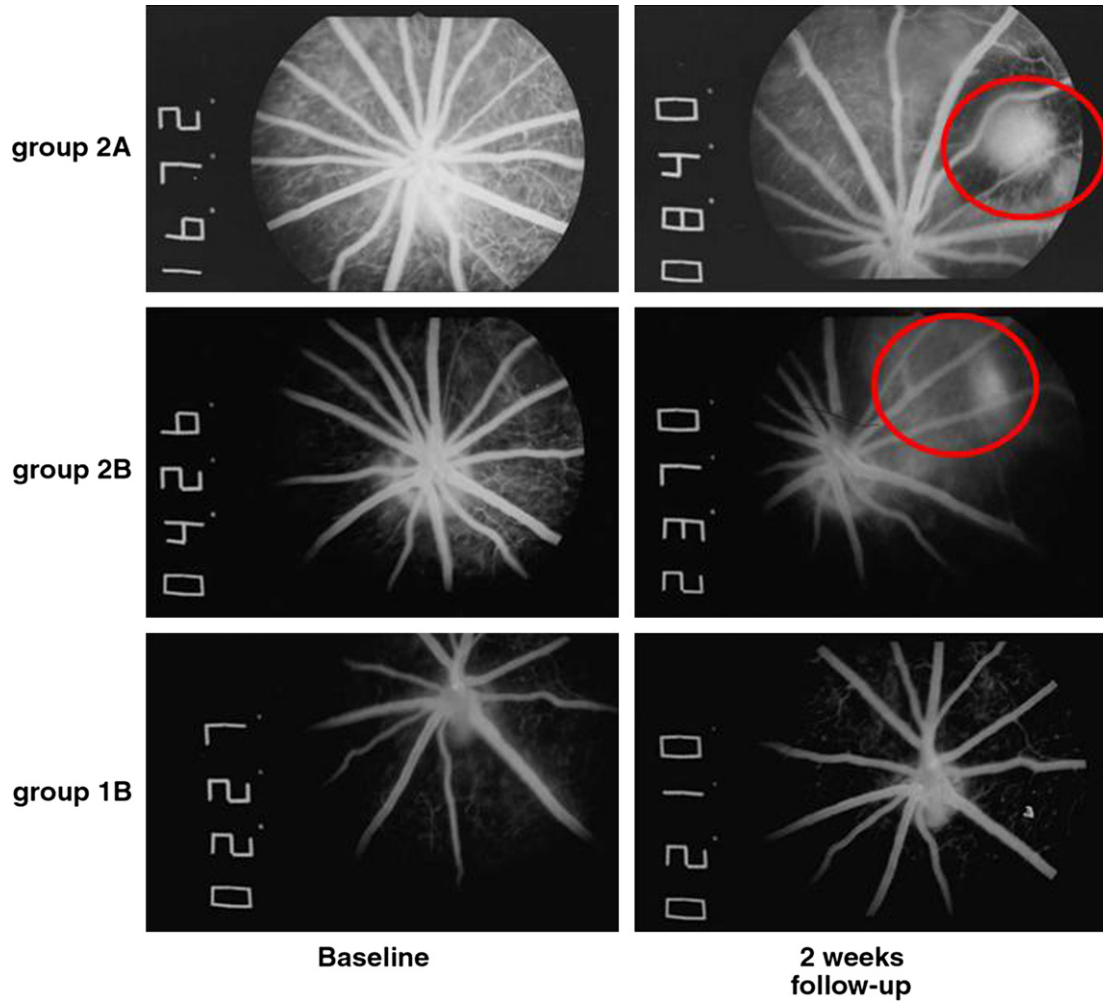
Fig. 4. Fluorescein angiography results. Group 2A: Hyperfluorescence area surrounded by hypofluorescence area. Group 2B: Large hyperfluorescence area. Group 1B: Normal fluorescein angiogram.

neovascularization (CNV), retinal leakage, or retinal vasculature non-perfusion specifically, and no signs in general of any damage to the retinal and choroidal vasculature.

ERG and electrical measurements suggest that no gross damage to either the retina or the electrode occurred during the experiment. Representative data are shown in Figs. 5 and
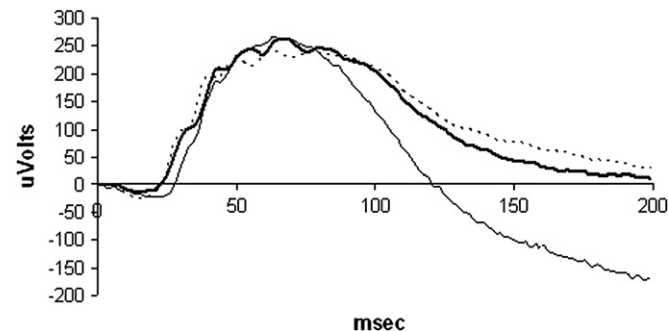

Fig. 5. Electroretinography after electrical stimulation. Rat maximal response ERG prior to stimulation (dashed line), Group 1C (thick solid line), and Group 2B (thin solid line). Traces are average of 15 bright flashes after 30 min dark adaptation.

6. In some rats, corneal haziness and vitreal hemorrhage was judged to be too severe to allow meaningful ERG. The electrode voltage was observed during all experiments. The waveform maintained the shape shown in Fig. 6 and did not change in a way that would indicate either gross failure of the electrode or saturation of the output due to compliance voltage limits. Pre- and post-stimulation measurements in a subset of electrodes show that the tissue resistance (high frequency impedance) changed on average -3.2% (range -12.9% to 4.2%, $n = 7$) and the charge storage capacity on average 0.5% (range -43% to 48%, $n = 10$). The stable tissue resistance indicates that the geometric surface area of the electrode changed minimally. The larger range of charge storage capacity indicates the formation or loss of an oxide layer during stimulation.

3.2. Histology

The histology in all sub-groups was analyzed by light microscopy (LM) in accordance with pre-established evaluation categories and grading scales for 18 observable anatomical features. An explanation of the grading scale is included as
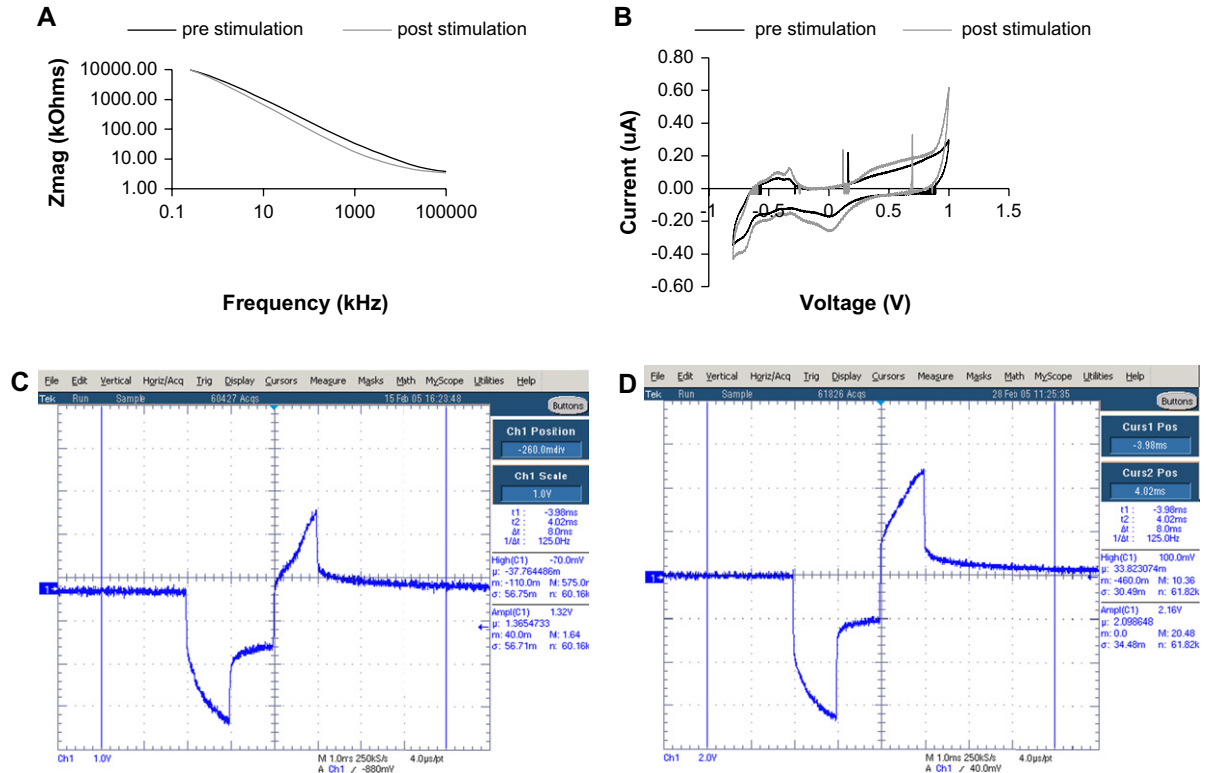
Fig. 6. Electrical evaluation of stimulating electrode. Impedance modulus spectrum (A) and cyclic voltammogram (B) before (solid) and after (dashed) pulsing indicate that the electrode was not significantly changed by stimulation. Voltage traces taken during 0.05 μC/phase (C) and 0.2 μC/phase (D) pulsing. Vertical scale: 1 V/major div (C) and 2 V/major div (D). Horizontal scale 1 ms/major div (C,D).

an appendix to the paper. Groups that were graded moderate to severe are summarized in Table 1.

Analysis of Groups 1A–C revealed minimal histological changes to the retina, RPE, and choriocapillaris. Observations include minimal inner retinal gliosis and focal decreased pigmentation of RPE. All other histological parameters evaluated showed no changes compared to control eyes. Subgroup 1A showed only minimal changes in the retina and RPE. The

changes included: gliosis (2 of 3 rats) and decreased pigmentation of RPE (3 of 3 rats). All other parameters evaluated were scored as zero (no change). Subgroup 1B showed only minimal changes in the retina and RPE. The changes included: gliosis (3 of 3 rats) and decreased pigmentation of RPE (1 of 3 rats). All other parameters evaluated were scored as zero. Subgroup 1C showed only minimal changes in the retina and RPE. The changes included: gliosis (4 of 6 rats) and decreased pigmentation of RPE (1 of 6 rats). All other parameters were scored as zero. Fig. 7 shows representative histological data from Group 1.

Subgroup 2A showed minimal, mild, moderate, or severe histological changes to the retina, RPE, and choriocapillaris. Moderate to severe reactions were noted in the outer plexiform layer thickness (3 of 4 rats), outer nuclear layer (4 of 4 rats), inner nuclear layer (1 of 4 rats), retinal gliosis (1 of 4 rats), loss of inner and outer segments of photoreceptors (4 of 4 rats), and choriocapillary atrophy (1 of 4 rats). All other parameters were scored as mild reaction or no change. The lesions were elliptical in shape and had a mean area of 0.096 ± 0.036 mm^2. Fig. 8A and B show tissue changes due mechanical pressure at the retina.

Subgroup 2B showed minimal, mild, moderate or severe histological changes to the retina, RPE, and choriocapillaris. Moderate and severe reactions were noted in the outer plexiform layer thickness (4 of 4 rats), outer nuclear layer (4 of 4 rats), inner and outer segment photoreceptors (4 of 4 rats),

Table 1
Significant pathological changes in Group 2

	Groups with moderate to severe reaction (number with moderate–severe/total number in sub-group)
Inner nuclear layer	Group 2A (1/4), Group 2B (1/4)
Thickness outer plexiform layer	Group 2A (4/4), Group 2B (4/4)
Pigmentary changes	Group 2B (3/4)
Gliosis	Group 2A (1/4)
ONL (Normal PR cells is 5–6 cells thick	Group 2A (4/4), Group 2B (4/4)
Photoreceptors inner segments	Group 2A (4/4), Group 2B (4/4)
Photoreceptors outer segments	Group 2A (4/4), Group 2B (4/4)
Decrease pigmentation	Group 2B (2/4)
RPE atrophy	Group 2B (1/4)
Chroriocapillary atrophy	Group 2A (1/4), Group 2B (1/4)
Large vessel choroidal atrophy	Group 2B (1/4)

Group 2A: Electrode touching retina without electrical stimulation. Group 2B: Electrode touching retina with electrical stimulation.
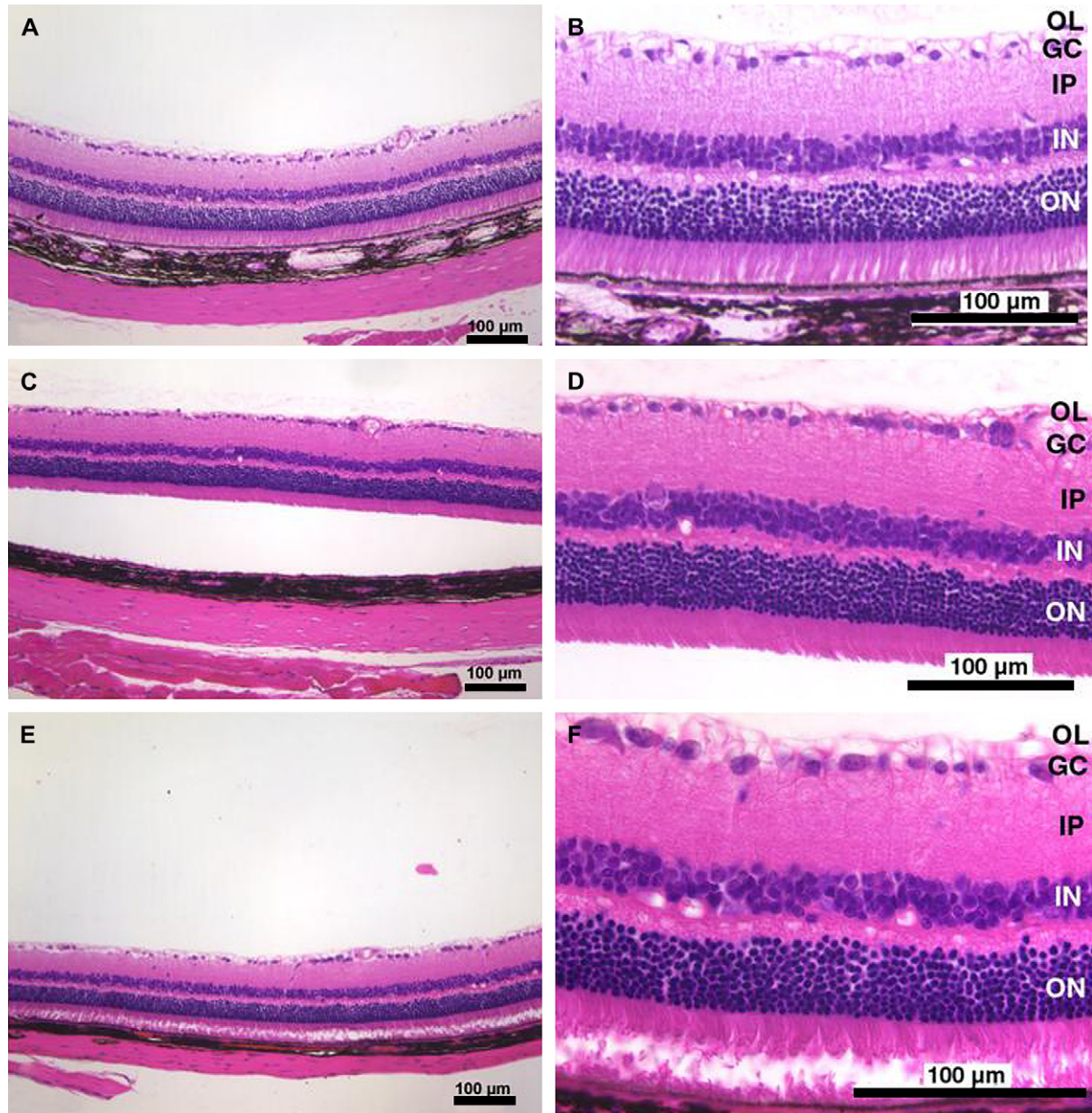
Fig. 7. Electrode in vitreous, not contacting the retina (Group 1). No significant damage to the retina was observed in any of the Group 1 experiments. The detachment observed (C, E) is a tissue processing artifact. OL, optic nerve layer; GC, ganglion cell; IP, inner plexiform layer; IN, inner nuclear layer; ON, outer nuclear layer. Bar = 100 μm.

inner nuclear layer (1 of 4 rats), pigmentary changes (3 of 4 rats), decreased RPE pigmentation (2 of 4 rats), RPE atrophy (1 of 4 rats), choriocapillaris atrophy (2 of 4 rats), and large vessel choroidal atrophy (1 of 4 rats). All other histological parameters were evaluated as mild or none. The lesions were elliptical in shape and had a mean area of 0.69 ± 0.41 mm^2. Fig. 8C and D show tissue changes seen at the retina due to mechanical pressure with electrical stimulation.

3.3. Statistical analysis

The comparison between groups with (Group 2) and without (Group 1) retinal contact showed significant differences in grading in all retinal, RPE, and choroid assessments ($p < 0.05$)

except INL thickness ($p = 0.28$). No significant difference was noted in retinal, RPE, or choroidal grading when comparing sub-groups with retinal contact and electrical stimulation (Group 2B) versus retinal contact alone (Group 2A). However, significant differences were noted in the area of the lesion in the retina (0.096 ± 0.036 vs. 0.69 ± 0.41 mm^2, $p < 0.05$).

3.4. Immunohistochemistry

GFAP staining was consistent with the LM findings. No GFAP upregulation was noted in control or in Group 1 rats. However, Group 2 rats did show increased expression of GFAP (Fig. 9).
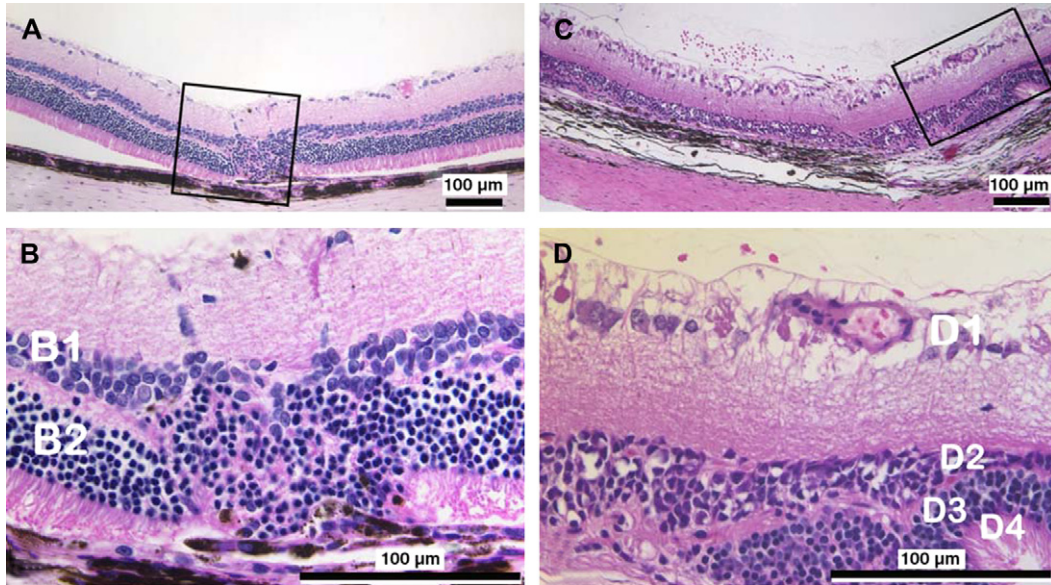
Fig. 8. Electrode contacting the retina (Group 2). (A, B) A focal lesion is present in case of retinal contact without electrical stimulation. (C, D) The lesion is larger when electrical stimulation is applied. A, C: low power image showing extent of lesion, B, D (same section): enlargement. Changes evident include Müller cell gliosis (D1), inner nuclear layer disorganization and thinning (B1, D2), outer nuclear layer disorganization (B2, D3) and photoreceptor rosette formation (D4). Bar = 100 μm.

4. Discussion

Neural damage from electrical stimulation has been investigated in other neural systems (McCreery et al., 1990, 1997) The principle of charge balanced stimulation was established over 40 years ago (Lilly and Sheer, 1961). Since then, a number of studies have investigated issues such as electrode materials for safe stimulation (Rose and Robblee, 1990; Weiland et al., 2002), neural injury from stimulation (Agnew et al., 1986), and neural survival with long-term stimulation (Leake
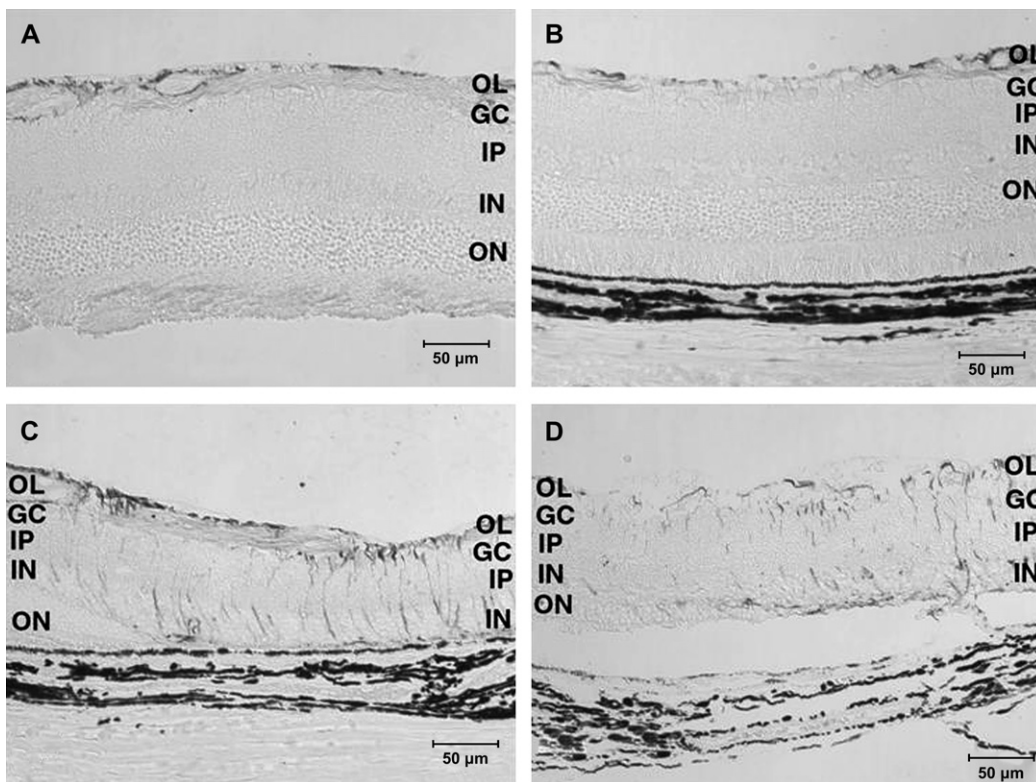

Fig. 9. Immunostaining for GFAP. Retinal cross sections are shown with GFAP labeled as black. (A) Group 1 (electrical stimulation, no contact): GFAP staining of astrocytes only. (B) Control eye (no surgery): no up-regulation of GFAP. (C) Group 2A and (D) Group 2B: glial reaction to retinal damage indicated by GFAP staining of Müller cells. OL, optic nerve layer; GC, ganglion cell; IP, inner plexiform layer; IN, inner nuclear layer; ON, outer nuclear layer. Bar = 50 μm.

et al., 2002). While this vast body of work can be used as a basis to begin examining the pathology of electrically stimulated retina, the unique cell types and structure of the retina warrant studies dedicated to understanding these effects in the retina. Understanding how electrical stimulation damages the retina is an important step in defining safe limits for electrical stimulation of the retina.

Retinal damage was greatest when the retina was directly contacted by the electrode, whether or not electrical stimulation was applied. The combination of retinal contact and electrical stimulation produced the most damage. Post-operative exams, including indirect examination, color photography and FA, suggest that in experiments with contact and electrical stimulation, CNV was created by the compression and stimulation of the retina. An interesting note in our results was that photoreceptors exhibited the most severe response to electrical stimulation, even though they were the furthest from the stimulating electrode. Since current density strength dissipates with distance from the electrode, the opposite might be expected, that is, the neural cells closest to the electrode would be subject to the high current density. Several possible explanations exist for this finding. The damage could be the result of an excitotoxic effect (Agnew et al., 1993). Some electrical stimulation studies have shown that the synapse between the bipolar cell and the photoreceptor is the most sensitive to electrical stimulation (Crapper and Noell, 1963). Continuous activation of this synapse by electrical stimulation could result in excess glutamate which is known to be neurotoxic. Alternatively, the photoreceptor damage could be secondary to RPE damage. The RPE has higher electrical resistivity than other retinal tissue (Heynen and van Norren, 1985) which may result in a greater voltage drop across the RPE and greater likelihood for electrical damage. However, RPE atrophy was only noted in 1 of 4 cases in Group 1B, which had exhibited the most severe photoreceptor damage.

Mechanical pressure alone produced damage. It is well known from retinal surgery that a momentary instrument touch to the retina can cause damage, possibly even a retinal tear that can lead to detachment. Photoreceptors showed the most damage in this sub-group, similar to the results from experiments with both pressure and electrical stimulation. Long-term retinal implant studies have shown that damage to the retina occurs where the greatest pressure is exerted by the stimulating array (Majji et al., 1999; Walter et al., 1999). Our results show that this damage can occur within 1 h of pressure, suggesting that retina implants need to be carefully positioned during surgery, since even the smallest pressure on the retina may cause permanent damage.

In contrast to the experiments where the electrode array contacted the retina, minimal retinal damage was evident when the electrode array was off the retina. It is possible that some of the stimulus current was shorted through the vitreous and out of the eye via low impedance paths such as the optic nerve or the cornea, or that the current density was sufficiently dissipated at the retina. It is important to restate that all the stimulus levels used in this study exceeded the accepted safe stimulation limits for platinum electrodes (0.35 mC/cm^2).

This was done intentionally since the goal of the experiment was to assess the retinal response to high charge density stimulation. Indeed, the electrode voltage plots in Fig. 6 demonstrate that the water window was exceeded, suggesting that harmful by-products were created from stimulation. However, only when the electrode was intimately contacting the retina was damage evident. This may be because stimulus was only applied for 1 h and the results of this study do not advocate applying the higher stimulus levels chronically. The results do suggest that the vitreous may provide a buffer for harmful reactants produced by electrical stimulation and that current flow in the eye is highly dependent on electrode proximity to the retina.

Minimal gliosis was noted in experiments without retinal contact, but this could be attributable to mechanical or inflammatory responses to insertion of the electrode into the vitreous. A study of penetrating ocular injury demonstrated increased pigment epithelium-derived factor due to needle penetration in rat (Penn et al., 2006), suggesting that surgical insult can trigger reactivity, even if the retina itself is not contacted. Our study only examined the tissue 2 weeks after stimulation. During this time, some healing may have taken place. No conclusions can be drawn about damage to the retina immediately after stimulation.

The exact position of the stimulating electrode in relation to the retina cannot be quantified for these experiments, which is an important consideration when interpreting the results. While it was clearly evident when the electrode was contacting the retina and when it was not, both the amount of contact and the separation when not contacting cannot be stated with certainty. While the exact distance cannot be quantified, the stimulating electrode was estimated to be within 0.5 mm of the retina. This is important because electrical field strength will dissipate rapidly with distance from the electrode, suggesting a possible explanation for the relative lack of damage when the electrode did not contact the retina, even though more than twice as much charge was used in some cases. This finding also suggests that electrodes closer to the retina may have a stricter safety limit to avoid retinal damage.

In summary, high charge density stimulation from an epiretinal electrode in normal rats damages photoreceptors more severely than the inner retina and ganglion cells. Moderate to severe changes were noted in the retina, RPE and choroid, only when the electrode was closely in contact with the retina. Contact with no electrical stimulation still resulted in retinal damage. The results imply that a successful retinal prosthesis design will consider carefully both electrical and mechanical safety issues.

Appendix. Supplementary material

Supplementary material associated with the article can be found, in the online version at doi:10.1016/j.exer.2007.02.014.

References

Agnew, W.F., Yuen, T.G.H., McCreery, D.B., Bullara, L.A., 1986. Histopathologic evaluation of prolonged intracortical electrical stimulation. Experimental Neurology 92, 162–185.

Agnew, W.F., McCreery, D.B., Yuen, T.G., Bullara, L.A., 1993. MK-801 protects against neuronal injury induced by electrical stimulation. Neuroscience 52 (1), 45–53.

Brummer, S.B., Robblee, L.S., Hambrecht, F.T., 1983. Criteria for selecting electrodes for electrical stimulation: theoretical and practical considerations. Ann.N.Y.Acad.Sci. 405, 159–171.

Crapper, D.R., Noell, W.K., 1963. Retinal excitation and inhibition from direct electrical stimulation. J. Neurophysiol. 26, 924–947.

Guven, D., Weiland, J.D., Fujii, G.Y., Mech, B.V., Mahadevappa, M., Greenberg, R., Roizenblatt, R., Qiu, G., Labree, L., Wang, X., Hinton, D., Humayun, M.S., 2005. Long-term stimulation by active epiretinal implants in normal and RCD1 dogs. J. Neural Eng. 2, 65–73.

Guven, D., Weiland, J.D., Maghribi, M., Davidson, J.C., Mahadevappa, M., Roizenblatt, R., Qiu, G., Krulevitz, P., Wang, X., Labree, L., Humayun, M.S., 2006. Implantation of an inactive epiretinal poly (di methyl) siloxane electrode arrays in dogs. Exp. Eye Res. 82, 81–89.

Heynen, H., van Norren, D., 1985. Origin of the electroretinogram in the intact macaque eye. II. Current source-density analysis. Vision Res. 25 (5), 709–715.

Hornig, R., Velikay-Parel, M., Feucht, M., Zehnder, T., Richard, G., 2006. Early Clinical Experience With A Chronic Retinal Implant System For Artificial Vision. ARVO, Ft. Lauderdale.

Humayun, M.S., Prince, M., de Juan Jr., E., Barron, Y., Moskowitz, M., Klock, I.B., Milam, A.H., 1999. Morphometric analysis of the extramacular retina from postmortem eyes with retinitis pigmentosa. Invest Ophthalmol Vis Sci 40 (1), 143–148.

Leake, P.A., Snyder, R.L., Hradek, G.T., 2002. Postnatal refinement of auditory nerve projections to the cochlear nucleus in cats. J. Comp. Neurol. 448 (1), 6–27.

Lilly, J.C., Sheer, D.E., 1961. Injury and Excitation by Electric Currents: The Balanced Pulse-Pair Waveform. Electrical Stimulation of the Brain, Hogg Foundation for Mental Health.

Mahadevappa, M., Weiland, J.D., Yanai, D., Fine, I., Greenberg, R.J., Humayun, M.S., 2005. Perceptual thresholds and electrode impedance in three retinal prosthesis subjects. IEEE Trans. Neural. Syst. Rehab. Eng. 13 (2), 201–206.

Majji, A.B., Humayun, M.S., Weiland, J.D., Suzuki, S., D'Anna, S.A., de Juan Jr., E., 1999. Long-term histological and electrophysiological results of an inactive epiretinal electrode array implantation in dogs. Invest. Ophthalmol. Vis. Sci. 40 (9), 2073–2081.

Marc, R.E., Jones, B.W., Watt, C.B., Strettoi, E., 2003. Neural remodeling in retinal degeneration. Prog. Retin. Eye Res. 22 (5), 607–655.

McCreery, D.B., Agnew, W.F., Yuen, T.G., Bullara, L.A., 1990. Charge density and charge per phase as cofactors in neural injury induced by electrical stimulation. IEEE Trans. Biomed. Eng. 37 (10), 996–1001.

McCreery, D.B., Yuen, T.G., Agnew, W.F., Bullara, L.A., 1997. A characterization of the effects on neuronal excitability due to prolonged microstimulation with chronically implanted microelectrodes. IEEE Trans. Biomed. Eng. 44 (10), 931–939.

Pardue, M.T., Phillips, M.J., Yin, H., Fernandez, A., Cheng, Y., Chow, A.Y., Ball, S.L., 2005. Possible sources of neuroprotection following subretinal silicon chip implantation in RCS rats. J. Neural. Eng. 2, 39–47.

Penn, J.S., McCollum, G.W., Barnett, J.M., Werdich, X.O., Koepke, K.A., Rajaratnam, V.S., 2006. Angiostatic effect of penetrating ocular injury: role of pigment epithelium-derived factor. Invest. Ophthalmol. Vis. Sci. 47 (1), 405–414.

Rizzo 3rd, J.F., Goldbaum, S., Shahin, M., Denison, T.J., Wyatt, J., 2004. In vivo electrical stimulation of rabbit retina with a microfabricated array: strategies to maximize responses for prospective assessment of stimulus efficacy and biocompatibility. Restor. Neurol. Neurosci. 22 (6), 429–443.

Rose, T.L., Robblee, L.S., 1990. Electrical stimulation with Pt electrodes. VIII. Electrochemically safe charge injection limits with 0.2 ms pulses. IEEE Trans. Biomed. Eng. 37 (11), 1118–1120.

Santos, A., Humayun, M.S., de Juan Jr., E., Greenberg, R.J., Marsh, M.J., Klock, I.B., Milam, A.H., 1997. Preservation of the inner retina in retinitis pigmentosa. A morphometric analysis. Arch. Ophthalmol. 115 (4), 511–515.

Sekirnjak, C., Hottowy, P., Sher, A., Dabrowski, W., Litke, A.M., Chichilnisky, E.J., 2006. Electrical stimulation of mammalian retinal ganglion cells with multi-electrode arrays. J. Neurophysiol. 95 (6), 3311–3326.

Shah, H.A., Montezuma, S.R., Rizzo 3rd, J.F., 2006. In vivo electrical stimulation of rabbit retina: Effect of stimulus duration and electrical field orientation. Exp. Eye Res. 83 (2), 247–254.

Stone, J.L., Barlow, W.E., Humayun, M.S., de Juan Jr., E., Milam, A.H., 1992. Morphometric analysis of macular photoreceptors and ganglion cells in retinas with retinitis pigmentosa. Arch. Ophthalmol. 110 (11), 1634–1639.

Walter, P., Szurman, P., Vobig, M., Berk, H., Ludtke-Handjery, H.C., Richter, H., Mittermayer, C., Heimann, K., Sellhaus, B., 1999. Successful long-term implantation of electrically inactive epiretinal microelectrode arrays in rabbits. Retina 19 (6), 546–552.

Weiland, J.D., Humayun, M.S., Anderson, D.J., 2002. In Vitro Electrical Properties for Iridium Oxide vs. Titanium Nitride Stimulating Electrodes. IEEE Trans. Biomed. Eng. 49 (12), 1574–1579.

Weiland, J.D., Liu, W., Humayun, M.S., 2005. Retinal prosthesis. Annu. Rev. Biomed. Eng. 7, 361–401.

Zrenner, E., 2002. Will retinal implants restore vision? Science 295 (5557), 1022–1025.

Zrenner, E., Besch, D., Bartz-Schmidt, K.U., Gekeler, F., Gabel, V.P., Kuttenkeuler, C., Sachs, H., Sailer, H., Wilhelm, B., Wilke, R., 2006. Subretinal Chronic Multi-Electrode Arrays Implanted in Blind Patients. ARVO, Ft. Lauderdale.